www.czasopisma.pan.pl PAN POLSKA AKADEMIA NAUK www.journals.pan.pl

Arch. Min. Sci. **67** (2022), 2, 303-316

Electronic version (in color) of this paper is available: http://mining.archives.pl

DOI: https://doi.org/10.24425/ams.2022.141460

YINGJIE CHANG[1], YOUZHI ZHANG[1*], DEQING GAN[1],
XINYI WANG[1], SHUANGCHENG DU[1],

CALCULATION MODEL OF PIPELINE RESISTANCE FOR CEMENTED PASTE BACKFILL CONSIDERING THIXOTROPY

The rheological behaviour of cemented paste backfill (CPB) has an important influence on the stability of its transportation in pipelines. In the present study, the time-dependent rheological behaviour of CPB was investigated to elucidate the effects of time and solid content. Experimental results showed that when CPB is subjected to a constant shear rate, the shear stress gradually decreases with time before finally stabilis ing. When the solid content was 60%~62%, a liquid network structure was the main factor that influenced the thixotropy of CPB, and the solid content had less influence. When the solid content was 64%~66%, a floc network structure was the main factor that influenced the thixotropy of CPB, and the solid content had a more significant influence on the thixotropy than the shear rate. The initial structural stability of CPB increased with the solid content, and this relationship can be described by a power function. Based on the experimental results, a calculation model of pipeline resistance considering thixotropy was proposed. The model was validated by using industrial experimental data. The current study can serve as a design reference for CPB pipeline transportation.

Keywords: thixotropy; cemented paste backfill; pipeline transportation; calculation model; hydraulic gradient

1. Introduction

Mining and mineral processing operations are associated with many challenges, such as surface subsidence and the accumulation of mining waste [1-4]. Cemented paste backfill (CPB) uses tailings to fill the underground extraction area, reducing the discharge of tailings and has become a mainstream mining practice in many countries [5-9]. CPB is usually prepared on the surface and then transported to the underground quarry, so it should have sufficient fluidity and

[1] NORTH CHINA UNIVERSITY OF SCIENCE AND TECHNOLOGY, COLLEGE OF MINING ENGINEERING, CHINA

* Corresponding author: zhangyouzhi@ncst.edu.cn

stability [10]. Determining rheological behaviour is essential for evaluating the fluidity and stability of CPB pipelines [11,12]. In fluid mechanics, yield stress and viscosity are essential parameters for characterising rheological behaviour [13]. Kretser et al. [14] reported that yield stress is a significant indicator for ensuring the successful startup of a pumping system from a static shutdown condition. Viscosity is an indicator of the subsequent pumping requirements and fluidity. However, these two parameters are not used in engineering terminology, and the fluidity of CPB is often assessed concerning the pipeline resistance.

Gao et al. [15] combined a structural fluid test with a particle flow model and proposed a method for optimising the conveying parameters of the CPB pipeline. They used the Herschel--Bulkley model to analyse the conveying resistance of CPB and established a function relating to the resistance and parameters. Bharathan et al. [16] discussed friction coefficient correlations for the hydraulic model and found that the Swamee-Aggarwal friction coefficient correlation can accurately predict the pressure loss along the CPB pipeline with an error within 5%. Cheng et al. [17] studied the influence of time and temperature on the rheological behaviour of CPB and proposed the time-temperature equivalent effect, which they used to establish a calculation model for the conveying resistance of the pipeline considering time and temperature [18]. Collected practical engineering cases of CPB from Gobi sand and tailings and proposed a flow loop test for estimating the pressure drop. They found that the Swamee-Aggarwal model can effectively predict the pressure drop for the laminar flow of a Bingham plastic fluid in the pipeline.

CPB is formed by mixing cement, tailings, and water into a paste with high solid content and non-Newtonian fluid behaviour [19-23]. Many researchers have investigated the rheological behaviour of CPB. Jiang et al. [24] investigated the effect of three mineral admixtures (i.e., fly ash, slag, and silica fume) on the rheological behaviour of CPB and found that partially replacing the cement with fly ash significantly improves the fluidity, as well as a linear correlation between the thixotropy and plastic viscosity. Guo et al. [25] used the theory of water film thickness to study the fluidity of CPB mixed with hydrotalcite and found that the bulk density of particles increases significantly with the amount of flocculant. Based on observations of inelastic suspended media, Dullaert and Mewis [26] established a general structural dynamics model describing the flow behaviour of thixotropic systems. Barnes [27] described the history of the development of thixotropy and its understanding by the scientific community today. Roussel et al. [28] found that the maximum critical strain is associated with colloidal interactions between cement particles, whereas the minimum critical strain is associated with early hydrates. Mewis and Wagner [29] classified and evaluated existing rheological models for thixotropic suspensions. Xue et al. [30] investigated the rheological behaviour of CPB made over time. It was from ultrafine tailings, and it determined the effects of high temperature, solid content, cement content, and binder type.

The rheological behaviour of CPB is consistent with the Bingham and Herschel-Buckley (H-B) models, but these models do not account for time dependence [31,32]. Time-dependent rheological behaviour has an important influence on the pipeline transportation of CPB [17,33,34]. Researchers have found that the yield stress and viscosity change over time [17,30,33], without accounting for the time dependence leads to inaccurate calculations of losses due to pipeline transmission resistance.

The objective of the present study was to clarify the coupling effect of time and solid content on the rheological behaviour of CPB. Experiments were performed with different solid contents and shear rates, and the evolution in the shear stress over time with different solid contents was analysed. A model was developed for calculating the pipeline resistance considering the effects of time and solid content on rheological behaviour and evaluated against industrial test data.

2. Materials and methods

2.1. Materials

CPB was mixed from unclassified tailings (i.e., all particle sizes) from Gaoguanying Iron Mine in Tangshan City, Hebei Province, China; P.O 42.5 Portland cement according to the China Common Portland Cement Standard; and tap water. A laser-diffraction particle size analyzer (Malvern) was used to detect the particle size distribution of the tailings and cement, which is shown in Fig. 1. The important particle size parameters for the unclassified tailings were d(50) = 13.37 μm and d(90) = 35.58 μm. The important particle size parameters for the cement were d(50) = 14.82 μm and d(90) = 42.94 μm. Table 1 presents the chemical composition of the tailings.

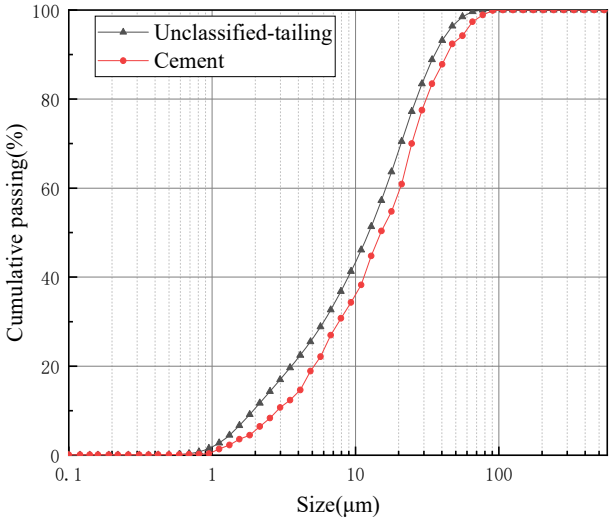

Fig. 1. Particle size distribution

TABLE 1

Chemical composition of tailings

Chemical composition	TFe	SiO_2	CaO	MgO	Al_2O_3	Others
Content (%)	6.00	67.58	4.04	5.60	7.30	9.48

2.2. Sample Preparation

The CPB experimental samples were prepared with a solid content of 60%, 62%, 64%, and 66% and a cement-tailing (c/t) ratio of 1:4. Previous exploratory experiments showed that these proportions resulted in good fluidity and stability. The cement, tailings, and tap water were poured into a container and then stirred for 3 min to produce the CPB samples.

2.3. Apparatus and experimental procedures

The thixotropic behaviour of CPB reflects the response of the internal structure to time and shear action [35,36]. Some scholars believe that the thixotropic area can indicate the structural buildup of cement paste [37]. However, the thixotropic area only provides a qualitative analysis of the thixotropic behaviour of CPB; it cannot provide an accurate calculation of the time-dependent rheological behaviour. Some researchers have found that shear stress curves with time can be obtained at a fixed shear rate and that two shear stresses can be obtained before and after thixotropy [38,39]. However, if regression analysis is applied to shear stress at multiple shear rates, the yield stress can be obtained, as shown in Fig. 2. The different transverse coordinates and shear stresses show the effects of time and shear rate on the rheological behaviour of CPB.

The rheological behaviour of CPB was tested using a rheometer (HAAKE Viscotester IQ) and a four-bladed rotor (FL22 4B/SS-01170440). After the material stabilised, the rotor was slowly placed in the sample. The test started with the controlled shear rate method. The change in shear stress with time was obtained by collecting data (i.e., shear rate, shear stress, and time) with a computerised monitoring system. The shear rate was set to 30 s^{-1}, 60 s^{-1}, 90 s^{-1}, and 120 s^{-1}, and the shear time was set to 1000 s. The measurement was repeated with reconstituted samples until a reproducible stable result was obtained.

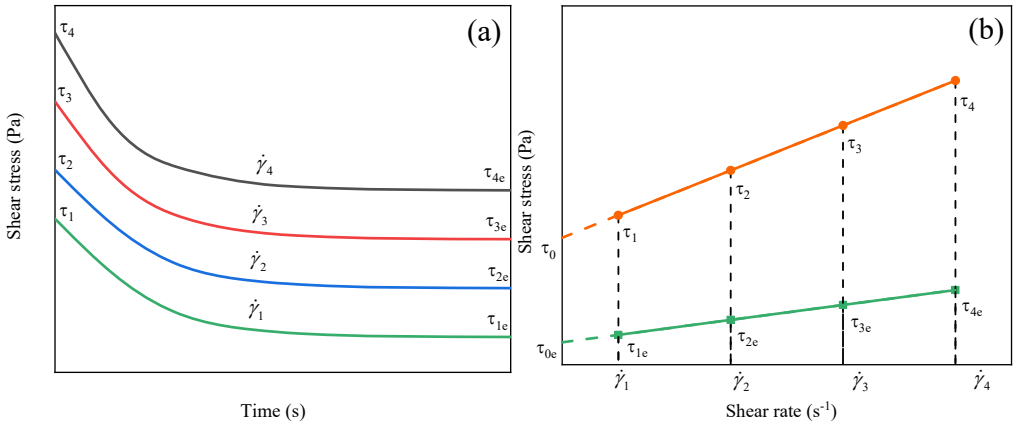

Fig. 2. Finding parameters of thixotropy by using a stress relaxation curve: (a) stress relaxation curve and (b) yield stress regression

3. Results and discussion

3.1. Effect of time and solid content on shear stress

Fig.3 shows the changes in shear stress of CPB with different solid content with time under the condition of a shear rate of 60 s^{-1}. As shown in Fig. 3(a), when the shear rate was fixed, the floc network structure of CPB was gradually destroyed with increasing shear time, and the shear stress gradually decreased. The shear stress stabilis ed at a certain value when the shear damage

and CPB recovery reached equilibrium. The rheological behaviour did not show significant time dependence at low solid contents. As the solid content increased, the internal particle content increased, which made the floc network structure more stable, and the shear stress increased.

The change in shear stress before and after thixotropy can be used to characterise CPB [30] and is given by

$$\Delta\tau = \tau_1 - \tau_2 \tag{1}$$

Where $\Delta\tau$ (Pa) is the change in shear stress, τ_1 (Pa) is the shear stress before thixotropy, and τ_2 (Pa) is the shear stress after thixotropy. Fig. 3(b) shows that increasing the solid content stabilised the internal floc network structure of the CPB and increased thixotropy. At solid contents of 60% and 62%, the high free water content meant that the liquid network was the main structure and thixotropic behaviour was not clear. After thixotropy, the change in shear stress increased from 39 to 50 Pa, using Eq. (2) to calculate the shear stress growth rate, which is 28%. When the solid content was 64% and 66%, the floc network was the main structure, and thixotropic behaviour produced qualitative change. After thixotropy, the shear stress increased from 159 to 375 Pa for a growth rate of 136%. Thus, the interparticle floc network structure was the main influence on the thixotropy of CPB.

$$p = \Delta\tau / \tau_1 \tag{2}$$

where p (%) is the growth rate, $\Delta\tau$ (Pa) is the change in shear stress, and τ_1 (Pa) is the shear stress before thixotropy.

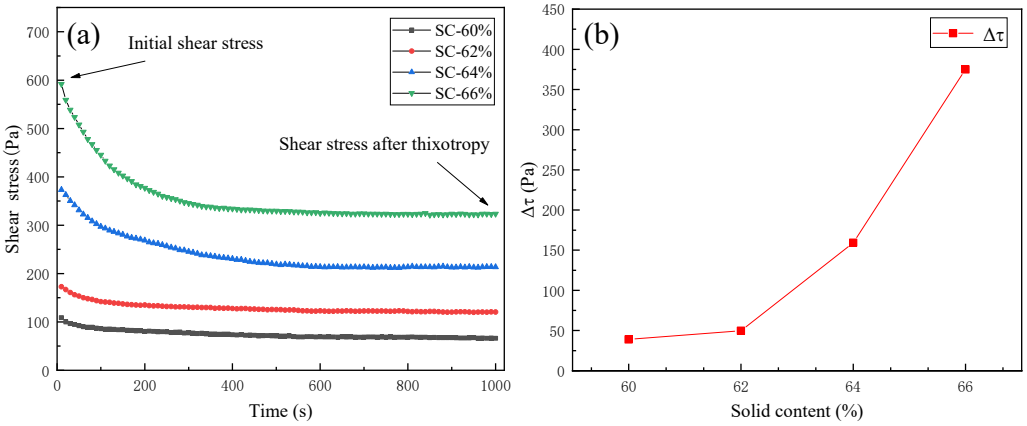

Fig. 3. Stress relaxation curves at different solid contents: (a) stress relaxation curve and (b) key parameters analysis

3.2. Effect of solid content on initial shear stress in CPB

The initial stress indicated the initial structural stability. Fig. 4 shows when the solid content is low, the interior of CPB is mainly a liquid network structure, and the liquid network structure is unstable, so the shear stress is low. With the increase of solid content, the content of solid

particles in CPB increases, and the floc network structure formed by solid particles increases, so the overall structure of the CPB is more stable and generates larger shear stress. Eq. (3) was used in regression analysis to obtain the relationship between the initial stress and solid content:

$$\tau_i = a \times c^m \tag{3}$$

where τ_i (Pa) is the initial stress, a and m are model parameters, and c (%) is the solid content. Table 2 presents the regression parameters.

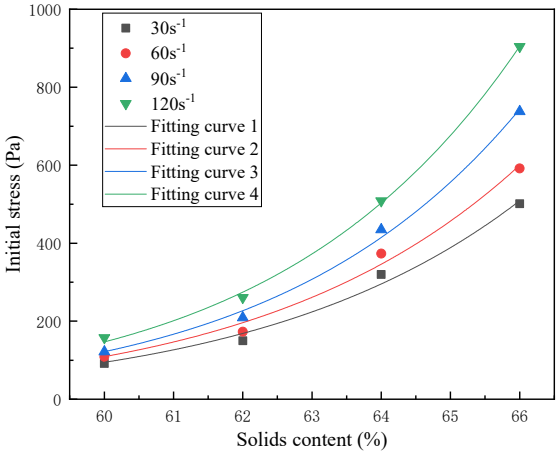

Fig. 4. Initial stress versus solid content

TABLE 2

Regression parameters

Shear rate (s^{-1})	a	m	R^2
30	3.8×10^{-30}	17.66	0.99
60	1.78×10^{-30}	17.88	0.99
90	2.14×10^{-32}	18.98	0.99
120	1.71×10^{-32}	19.08	0.99

3.3. Effect of shear rate on shear stress

As shown in Fig. 5(a), with the increase in shearing time, the internal structure of CPB is gradually destroyed, resulting in a gradual decrease of shear stress, and when the equilibrium between failure and recovery is reached, the shear stress remains stable. When the shear rate is large, the CPB is subjected to a large shearing action, resulting in a large shear stress. From Fig. 5(b), with the increase in shear rate, CPB is subjected to greater shearing action, and the internal floc network structure is damaged more seriously, so the change of shear stress is greater. When the shear rate was increased from 90 to 120 s^{-1}, the change in stress increased from 375 to 497 Pa for a growth rate of only 33%. This indicates that the shear rate has less influence on the thixotropy of CPB than the solid content.

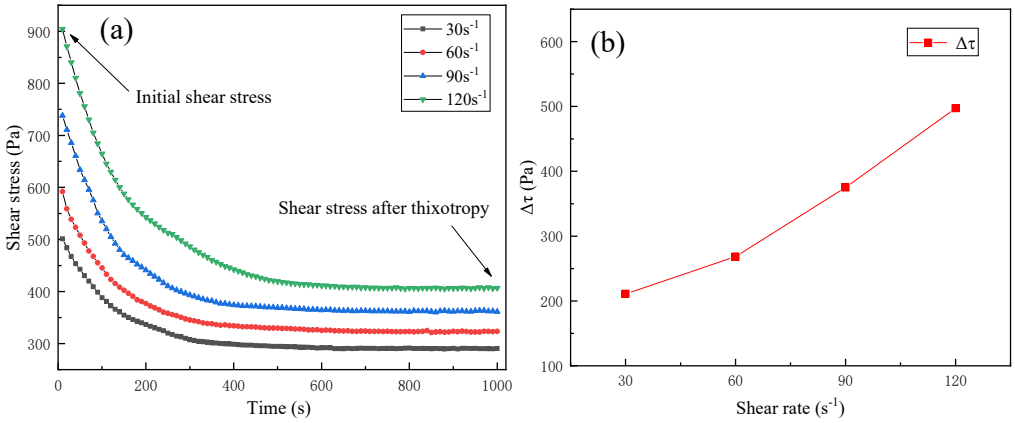

Fig. 5. Stress relaxation curves at different shear rates (solid content of 66%): (a) stress relaxation curves and (b) analysis of key parameters

3.4. Coupling effect of time and solid content on rheological behaviour

CPB is commonly regarded as a Bingham fluid. Thus, the resulting rheological curve (Fig. 6) was regressed by using the Bingham model [30], which is given by

$$\tau = \tau_0 + \eta\dot{\gamma} \tag{4}$$

where τ (Pa) is the shear stress, τ_0 (Pa) is the yield stress, η (Pa·s) is the plastic viscosity, and $\dot{\gamma}$ (s^{-1}) is the shear rate.

To optimise the amount of data, a point was selected every 100 s for regression analysis. In total, 44 regression analyses were performed. The yield stress and plastic viscosity were obtained at different times.

Fig. 7 shows the yield stress and plastic viscosity curves over time with different solid contents. As the shear time increased, the yield stress and plastic viscosity gradually decreased and then stabilised.

The changes in the yield stress and plastic viscosity over time were observed to show similar patterns. Eq. (5) was constructed to characterise the change in yield stress over time:

$$\tau_0 = k_1 + k_2 \times k_3^t \tag{5}$$

where τ_0 (Pa) is the yield stress, k_1, k_2 and k_3 are regression parameters related to the yield stress, and t (s) is the time. Table 3 presents the regression parameters of the yield stress.

Eq. (6) was constructed to characterise the change in plastic viscosity over time:

$$\eta = s_1 + s_2 \times s_3^t \tag{6}$$

where η (Pa·s) is the plastic viscosity, s_1, s_2 and s_3 are regression parameters related to the plastic viscosity, and t (s) is the time. Table 4 presents the regression parameters of the plastic viscosity.

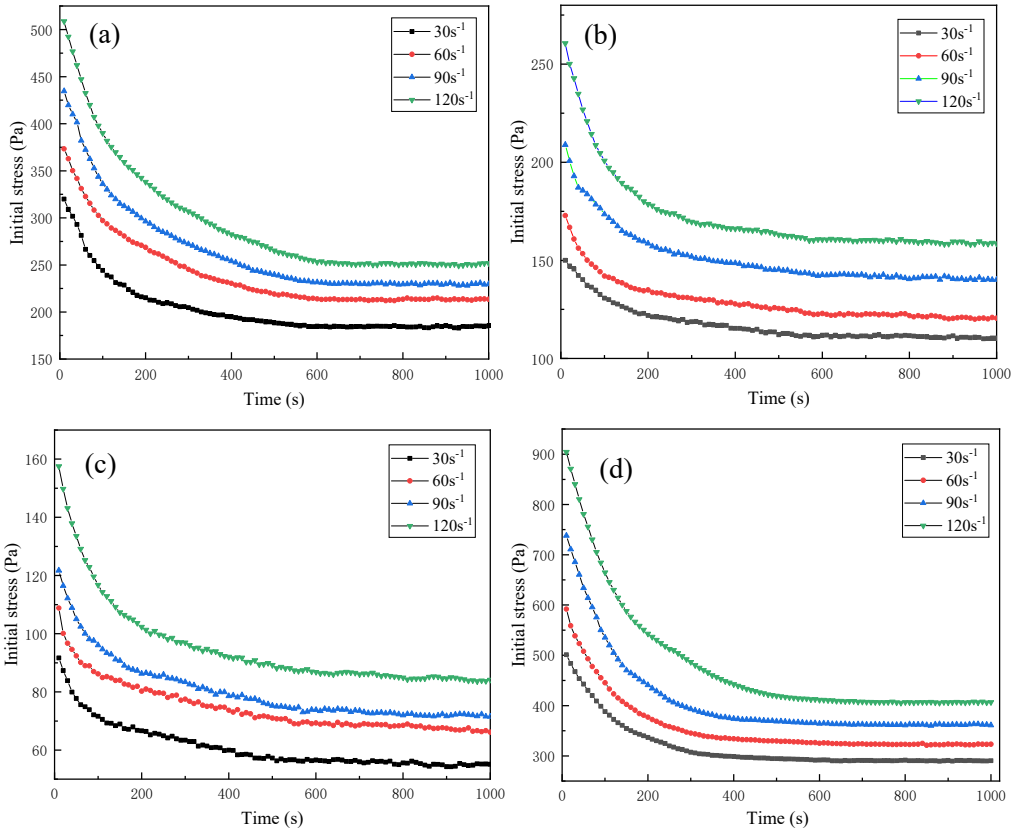

Fig. 6. Stress relaxation curves at different solid content: (a) 60%, (b) 62%, (c) 64% and (d) 66%

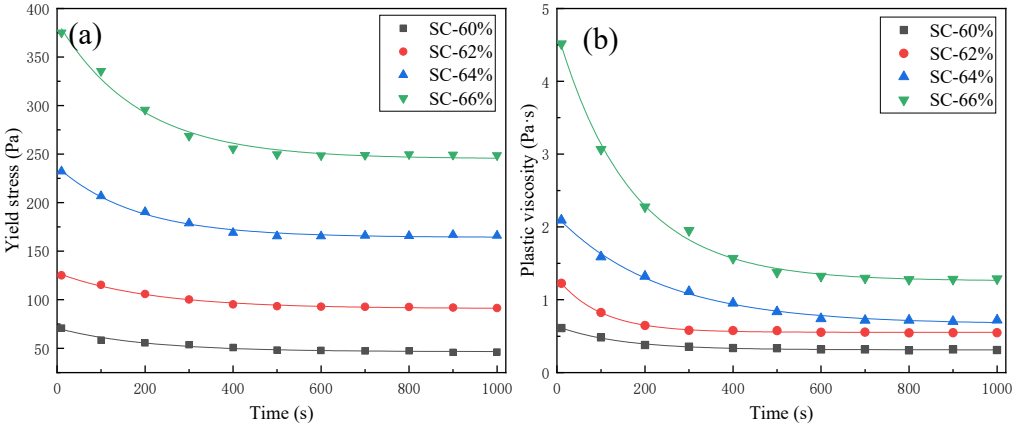

Fig. 7. Curves of the (a) yield stress and (b) plastic viscosity with time

TABLE 3

Regression parameters of the yield stress with time

Solid content (%)	k_1	k_2	k_3	R^2
60	46.47	24.26	0.99	0.97
62	91.66	36.79	0.99	0.99
64	163.44	74.38	0.99	0.99
66	245.37	140.98	0.99	0.98

TABLE 4

Regression parameters of the plastic viscosity with time

Solid content (%)	s_1	s_2	s_3	R^2
60	0.31	0.32	0.99	0.99
62	0.55	0.75	0.99	0.99
64	0.66	1.47	0.99	0.99
66	1.26	2.56	0.99	0.99

Correlation analysis revealed strong correlations between the solid content and the parameters k_1, k_2, s_1, and s_2. Meanwhile, k_3 and s_3 were constants independent of the solid content, as shown in Fig. 8. The relationships between the regression parameters and solid content are given in Eqs. (7)-(10):

$$k_1 = 2.29c^2 - 255.90c + 7133.36 \tag{7}$$

$$k_2 = 3.38c^2 - 406.42c + 12243.53 \tag{8}$$

$$s_1 = 0.016c^2 - 1.88c + 55.26 \tag{9}$$

$$s_2 = 0.05c^2 - 5.95c + 177.40 \tag{10}$$

where k_1 and k_2 are regression parameters related to the yield stress, s_1 and s_2 are regression parameters related to the plastic viscosity, and c (%) is the solid content. The correlation coefficients R^2 for the regression parameters k_1, k_2, s_1, and s_2 were 0.99, 0.99, 0.96, and 0.99, respectively, which indicates high correlation. Eqs. (7) and (8) were substituted into Eq. (5) to obtain the coupling effect of time and solid content on the yield stress:

$$\tau_0 = 2.29c^2 - 255.90c + (3.38c^2 - 406.42c + 12243.53) \times 0.99^t + 7133.36 \tag{11}$$

Eqs. (9) and (10) were substituted into Eq. (6) to obtain the coupling effect of time and solid content on the plastic viscosity:

$$\eta = 0.016c^2 - 1.88c + (0.05c^2 - 5.95c + 177.40) \times 0.99^t + 55.26 \tag{12}$$

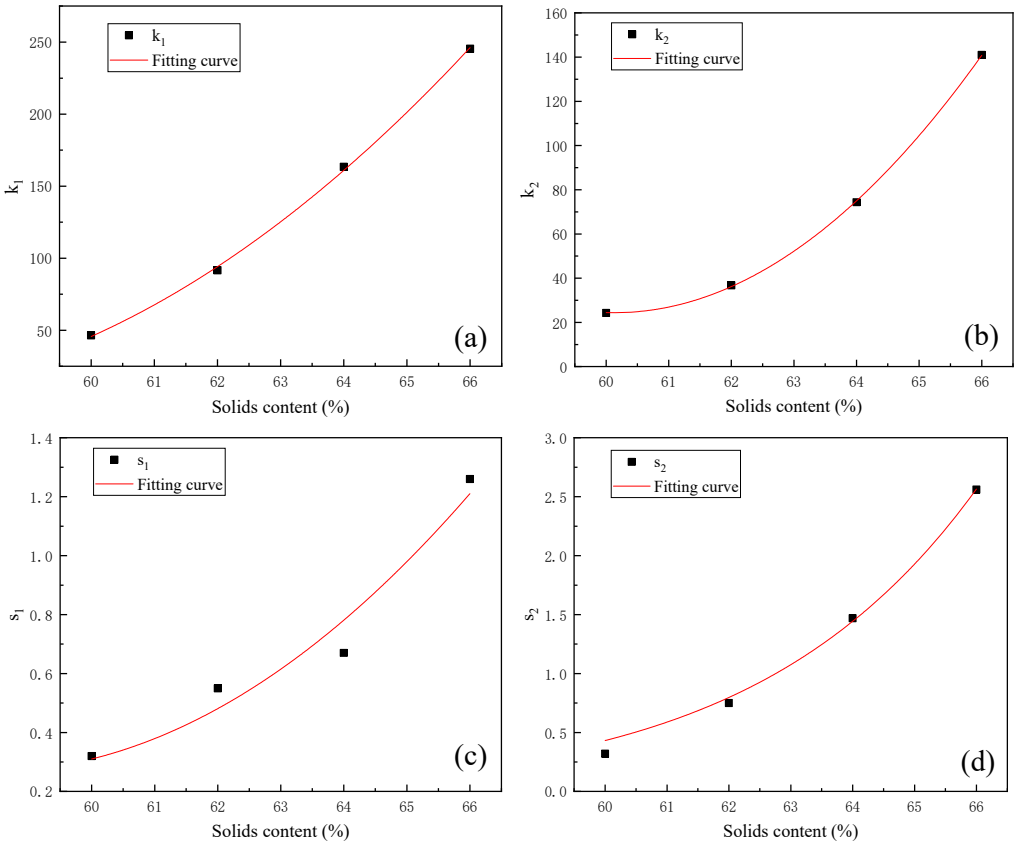

Fig. 8. Regression parameters versus solid content. (a) k_1 versus solid content, (b) k_2 versus solid content, (c) s_1 versus solid content, and (d) s_2 versus solid content

3.5. Coupling effect of time and solid content on pipeline resistance

3.5.1. Calculation model

The Bingham equation expresses the relationship between the rheological parameters and pipeline resistance. The pipeline resistance can be calculated as follows [39-41]:

$$i = \frac{16}{3D}\tau_0 + \frac{32v}{D^2}\eta \tag{13}$$

However, Eq. (13) does not consider the effect of thixotropy on the rheological behaviour of CPB. Eqs. (11) and (12) were inserted into Eq. (13) to obtain an equation for calculating the pipeline resistance considering time and solid content:

$$i = \frac{16}{3D}\left\{2.29c^2 - 255.90c + (3.38c^2 - 406.42c + 12243.53) \times 0.99^t + 7133.36\right\} + \frac{32v}{D^2}\left\{0.016c^2 - 1.88c + \left(0.05c^2 - 5.95c + 177.40\right) \times 0.99^t + 55.26\right\} \quad (14)$$

3.5.2. Model applicability

Experimental data were collected from the literature to verify the applicability of the proposed model given by Eq. (14) [42]. The solid content was 70%, the pipe diameter was 150 mm, and the pipe length was 250 m. Then, the Bingham equation and Eq. (14) were each used to calculate the pipeline resistance. However, the hydraulic gradient calculated by Eq. (14) is a variable value, so Eq. (15) is used to calculate the average hydraulic gradient. The average hydraulic gradient was calculated as follows:

$$i_a = \frac{\sum_{k=1}^{n} i_k}{n} \quad (15)$$

where i_a (Pa·m^{-1}) is the average hydraulic gradient, i_k (Pa·m^{-1}) is the hydraulic gradient at certain intervals, and n is the number of hydraulic gradient calculations.

Table 5 presents the results. Some errors were observed because of the different materials used. The Bingham equation had an average error of 57.82%, whereas Eq. (14) had an average error of 32.91%. Thus, the proposed model was demonstrated to be more accurate than the Bingham equation. When the flow rate was low, Eq. (14) resulted in a larger error than the Bingham equation. When the flow rate was large, Eq. (14) resulted in a smaller error than the Bingham equation. This can be explained by the thixotropic behaviour of CPB being more pronounced at higher flow rates. Therefore, the proposed model is suitable for working conditions with high flow rates.

TABLE 5

Hydraulic gradient calculation results

Velocity (m·s^{-1})	Measured values (Pa·m^{-1})	Bingham equation (Pa·m^{-1})	Error value (%)	Average error (%)	Eq. (14) (Pa·m^{-1})	Error value (%)	Average error (%)
0.70	3932.00	3662.59	6.84	57.82	2361.83	39.94	32.91
1.40	4709.00	6772.25	43.81		4995.45	6.07	
2.10	5612.00	9881.91	76.07		7257.78	29.32	
2.80	6351.00	12991.57	104.55		9926.84	56.30	

4. Conclusions

The present study investigated the influence of time and solid content on the rheological behaviour of CPB. A calculation model was developed that considers the coupling effect of time and solid content on the pipeline resistance. The main conclusions are as follows:

(1) At a constant shear rate, the shear stress gradually decreased with time and eventually stabilised. When the solid content is constant, the greater the shear rate, the greater the shear stress.
(2) In the range of solid content of 60%~66%, the thixotropy of CPB is mainly affected by the solid content. When the solid content is low, the thixotropy of CPB is small, and when the solid content is high, the thixotropy is large. The yield stress and plastic viscosity gradually decreased with increasing shear time and eventually stabilised.
(3) A model based on the Bingham equation was developed for calculating the resistance to pipeline transportation considering thixotropy and validated. According to the calculation results, the model in this paper is more suitable for the calculation of pipeline transportation resistance of CPB with a high concentration and flow rate of 1~2 m/s, and has certain reference significance for mine filling under this working condition.

Despite the obtained results, there are still some limitations due to the limitation of materials. Further research is necessary to investigate the effect of thixotropy on the rheological behaviour of CPB. Future work is required to investigate the mechanisms of thixotropy at the microscale and to develop numerical models for quantitative analysis of the thixotropy of CPB.

Acknowledgments

This research was supported by the National Natural Science Foundation of China (Nos. 51774137); Natural Science Foundation of Hebei Province, China (No. E2019209326).

References

[1] M. Benzaazoua, B. Bussiere, I. Demers, M. Aubertin, E. Fried, A. Blier, Integrated mine tailings management by combining environmental desulphurization and cemented paste backfill: Application to mine Doyon, Quebec, Canada. Miner. Eng. **21**, 4, 330-340 (2008). DOI: https://doi.org/10.1016/j.mineng.2007.11.012

[2] X. Zhao, A. Fourie, C.C. Qi, Mechanics and safety issues in tailing-based backfill: A review. International Journal of Minerals Metallurgy and Materials **27**, 9, 1165-1178 (2020). DOI: https://doi.org/10.1007/s12613-020-2004-5

[3] D.M. Huang, D.Q. Xing, X.K. Chang, Y.Y. Zhu, C.J. Gao, Analysis and application of filling mining technology in china's mining area: A case study of yuxing coal mine. Arch. Min. Sci. **66**, 4, 611-624 (2021). DOI: https://doi.org/10.24425/ams.2021.139600

[4] W.B. Xing, W.P. Huang, F. Feng, Research on application of strip backfilling mining technology – a case study. Arch. Min. Sci. **66**, 4, 595-609 (2021). DOI: https://doi.org/10.24425/ams.2021.139599

[5] H.Z. Jiao, S.F. Wang, Y.X. Yang, X.M. Chen, Water recovery improvement by shearing of gravity-thickened tailings for cemented paste backfill. J. Cleaner. Prod. **245**, (2020). DOI: https://doi.org/10.1016/j.jclepro.2019.118882

[6] L. Orejarena, M. Fall, Artificial neural network based modeling of the coupled effect of sulphate and temperature on the strength of cemented paste backfill. CaJCE **38**, 1, 100-109 (2011). DOI: https://doi.org/10.1139/l10-109

[7] K. Klein, D. Simon, Effect of specimen composition on the strength development in cemented paste backfill. CaGeJ **43**, 3, 310-324 (2006). DOI: https://doi.org/10.1139/t06-005

[8] W.C. Li, M. Fall, Sulphate effect on the early age strength and self-desiccation of cemented paste backfill. Constr. Build. Mater. **106**, 296-304 (2016). DOI: https://doi.org/10.1016/j.conbuildmat.2015.12.124

[9] H.Z. Jiao, S.F. Wang, A.X. Wu, H.M. Shen, J.D. Wang, Cementitious property of NaAlO2-activated Ge slag as cement supplement. International Journal of Minerals Metallurgy and Materials **26**, 12, 1594-1603 (2019). DOI: https://doi.org/10.1007/s12613-019-1901-y

[10] D. Wu, S.J. Cai, G. Huang, Coupled effect of cement hydration and temperature on rheological properties of fresh cemented tailings backfill slurry. Transactions of Nonferrous Metals Society of China **24**, 9, 2954-2963 (2014). DOI: https://doi.org/10.1016/s1003-6326(14)63431-2

[11] Q.D. Nguyen, D.V. Boger. Application of rheology to solving tailings disposal problems. Int. J. Miner. Process **54**, 3-4, 217-233 (1998). DOI: https://doi.org/10.1016/s0301-7516(98)00011-8

[12] N. Gharib, B. Bharathan, L. Amiri, M. McGuinness, F.P. Hassani, A.P. Sasmito, Flow characteristics and wear prediction of Herschel-Bulkley non-Newtonian paste backfill in pipe elbows. CJChE **95**, 6, 1181-1191 (2017). DOI: https://doi.org/10.1002/cjce.22749

[13] Q.S. Chen, Q.L. Zhang, X.M. Wang, C.C. Xiao, Q. Hu, A hydraulic gradient model of paste-like crude tailings backfill slurry transported by a pipeline system. Environmental Earth Sciences **75**, 14 (2016). DOI: https://doi.org/10.1007/s12665-016-5895-8

[14] R. deKretser, P.J. Scales, D.V. Boger, Improving clay-based tailings disposal: Case study on coal tailings. AIChE **43**, 7, 1894-1903 (1997). DOI: https://doi.org/10.1002/aic.690430724

[15] R.G. Gao, K.P. Zhou, Y.L. Zhou, C. Yang, Research on the fluid characteristics of cemented backfill pipeline transportation of mineral processing tailings. Alexandria Engineering Journal **59**, 6, 4409-4426 (2020). DOI: https://doi.org/10.1016/j.aej.2020.07.047

[16] B. Bharathan, M. McGuinness, S. Kuhar, M. Kermani, F.P. Hassani, A.P. Sasmito, Pressure loss and friction factor in non-Newtonian mine paste backfill: Modelling, loop test and mine field data. Powder Technol. **344**, 443-453 (2019). DOI: https://doi.org/10.1016/j.powtec.2018.12.029

[17] H.Y. Cheng, S.C. Wu, H. Li, X.Q. Zhang, Influence of time and temperature on rheology and flow performance of cemented paste backfill. Constr. Build. Mater. **231** (2020). DOI: https://doi.org/10.1016/j.conbuildmat.2019.117117

[18] X.B. Yang, B.L. Xiao, Q. Gao, J.Y. He, Determining the pressure drop of cemented Gobi sand and tailings paste backfill in a pipe flow. Constr. Build. Mater. **255** (2020). DOI: https://doi.org/10.1016/j.conbuildmat.2020.119371

[19] D. Wu, M. Fall, S.-J. Cai, Coupled Modeling of Temperature Distribution and Evolution in Cemented Tailings Backfill Structures that Contain Mineral Admixtures. Geotech. Geol. Eng. **30**, 4 (2012)

[20] A.X. Wu, Y. Wang, H.J. Wang, S.H. Yin, X.X. Miao, Coupled effects of cement type and water quality on the properties of cemented paste backfill. Int. J. Miner. Process **143**, 65-71 (2015). DOI: https://doi.org/10.1016/j.minpro.2015.09.004

[21] N. Cruz, Y.J. Peng, Rheology measurements for flotation slurries with high clay contents – A critical review. Miner. Eng. **98**, 137-150 (2016). DOI: https://doi.org/10.1016/j.mineng.2016.08.011

[22] D. Wu, R.K. Zhao, C.W. Xie, S. Liu, Effect of curing humidity on performance of cemented paste backfill. International Journal of Minerals Metallurgy and Materials **27**, 8, 1046-1053 (2020). DOI: https://doi.org/10.1007/s12613-020-1970-y

[23] S. Cao, E. Yilmaz, W.D. Song, Evaluation of Viscosity, Strength and Microstructural Properties of Cemented Tailings Backfill. Minerals **8**, 8 (2018). DOI: https://doi.org/ARTN 35210.3390/min8080352

[24] H.Q. Jiang, M. Fall, E. Yilmaz, Y.H. Li, L. Yang, Effect of mineral admixtures on flow properties of fresh cemented paste backfill: Assessment of time dependency and thixotropy. Powder Technol. **372**, 258-266 (2020). DOI: https://doi.org/10.1016/j.powtec.2020.06.009

[25] Z.B. Guo, J.P. Qiu, H.Q. Jiang, J. Xing, X.G. Sun, Z.Y. Ma. Flowability of ultrafine-tailings cemented paste backfill incorporating superplasticizer: Insight from water film thickness theory. Powder Technol. **381**, 509-517 (2021). DOI: https://doi.org/10.1016/j.powtec.2020.12.035

[26] K. Dullaert, J. Mewis, A structural kinetics model for thixotropy. J. Non-Newtonian Fluid Mech. **139**, 1-2, 21-30 (2006). DOI: https://doi.org/10.1016/j.jnnfm.2006.06.002

[27] H.A. Barnes, Thixotropy – A review. J. Non-Newtonian Fluid Mech. **70**, 1-2, 1-33 (1997). DOI: https://doi.org/10.1016/s0377-0257(97)00004-9

[28] N. Roussel, G. Ovarlez, S. Garrault, C. Brumaud, The origins of thixotropy of fresh cement pastes. Cem. Concr. Res. **42**, 1, 148-157 (2012). DOI: https://doi.org/10.1016/j.cemconres.2011.09.004

[29] J. Mewis, N.J. Wagner, Thixotropy. Adv. Colloid. Interface Sci. **147-48**, 214-227 (2009). DOI: https://doi.org/10.1016/j.cis.2008.09.005

[30] Z.L. Xue, D.Q. Gan, Y.Z. Zhang, Z.Y. Liu, Rheological behavior of ultrafine-tailings cemented paste backfill in high-temperature mining conditions. Constr. Build. Mater. **253** (2020). DOI: https://doi.org/10.1016/j.conbuildmat.2020.119212

[31] S. Lim, K.H. Ahn, S.J. Lee, A. Kumar, N. Duan, X.D. Sun, et al., Yield and flow measurement of fine and coarse binary particulate mineral slurries. Int. J. Miner. Process **119**, 6-15 (2013). DOI: https://doi.org/10.1016/j.minpro.2012.12.009

[32] X.M. Wang, J.X. Li, Z.Z. Xiao, W.G. Xiao, Rheological properties of tailing paste slurry. Journal of Central South University of Technology **11**, 1, 75-79 (2004). DOI: https://doi.org/10.1007/s11771-004-0016-3

[33] X.J. Deng, B. Klein, J.X. Zhang, D. Hallbom, B. de Wit, Time-dependent rheological behaviour of cemented backfill mixture. International Journal of Mining Reclamation and Environment **32**, 3, 145-162 (2018). DOI: https://doi.org/10.1080/17480930.2016.1239305

[34] D. Simon, M. Grabinsky, Apparent yield stress measurement in cemented paste backfill. International Journal of Mining Reclamation and Environment **27**, 4, 231-256 (2013). DOI: https://doi.org/10.1080/17480930.2012.680754

[35] R. Neelakantan, G.F. Vaezi, R.S. Sanders, Effect of shear on the yield stress and aggregate structure of flocculant-dosed, concentrated kaolinite suspensions. Miner. Eng. **123**, 95-103 (2018). DOI: https://doi.org/10.1016/j.mineng.2018.03.016

[36] X. Li, Z.C. Grasley, E.J. Garboczi, J.W. Bullard, Simulation of the influence of intrinsic C-S-H aging on time-dependent relaxation of hydrating cement paste. Constr. Build. Mater. **157**, 1024-1031 (2017). DOI: https://doi.org/10.1016/j.conbuildmat.2017.09.178

[37] Q. Yuan, D.J. Zhou, B.Y. Li, H. Huang, C.J. Shi, Effect of mineral admixtures on the structural build-up of cement paste. Constr. Build. Mater. **160**, 117-126 (2018). DOI: https://doi.org/10.1016/j.conbuildmat.2017.11.050

[38] Y. Qian, S. Kawashima, Use of creep recovery protocol to measure static yield stress and structural rebuilding of fresh cement pastes. Cem. Concr. Res. **90**, 73-79 (2016). DOI: https://doi.org/10.1016/j.cemconres.2016.09.005

[39] M.Z. He, Y.M. Wang, E. Forssberg, Slurry rheology in wet ultrafine grinding of industrial minerals: a review. Powder Technol. **147**, 1-3, 94-112 (2004). DOI: https://doi.org/10.1016/j.powtec.2004.09.032

[40] M.Z. Li, Y.P. He, Y.D. Liu, C. Huang, Effect of interaction of particles with different sizes on particle kinetics in multi-sized slurry transport by pipeline. Powder Technol. **338**, 915-930 (2018). DOI: https://doi.org/10.1016/j.powtec.2018.07.088

[41] J. Sobota, J.X. Xia, E. Kirichenko, Dynamic states equations of transport pipeline in deep-sea mining. Arch. Min. Sci. **66**, 3, 385-392 (2021). DOI: https://doi.org/10.24425/ams.2021.138595

[42] J.W. Bian, Q.L. Zhang, H. Wang, Pipeline hydraulic gradient model of paste-like based on L-pipe experiments. Journal of China University of Mining and Technology **48**, 1, 23-28 (2019). (in Chinese) doi:10.13247/j.cnki.jcumt.000962